Studies of NO Adsorption on Pt(110)-(1×2) and (1×1) Surfaces Using Density Functional Theory

Hideo Orita,*,† Isao Nakamura,‡ and Tadahiro Fujitani‡

Research Institute for Innovation in Sustainable Chemistry, National Institute of Advanced Industrial Science and Technology (AIST), Tsukuba Central 5, 1-1-1 Higashi, Tsukuba, Ibaraki 305-8565, Japan, and Research Institute for Innovation in Sustainable Chemistry, National Institute of Advanced Industrial Science and Technology (AIST), 16-1 Onogawa, Tsukuba, Ibaraki 305-8569, Japan

Received: February 16, 2005; In Final Form: March 26, 2005

Adsorption of NO on Pt(110)-(1×2) and (1×1) surfaces has been investigated by density functional theory (DFT) method (periodic DMol^3) with full geometry optimization and without symmetry restriction. Adsorption energies, structures, and N−O stretching vibrational frequencies of NO are studied by considering multiple possible adsorption sites and comparing with the experimental data. Adsorption is strongly dependent on both coverage and surface phase. The assignment of adsorption sites has been carried out with precise calculation of vibrational frequencies for NO on various sites. We clearly show the NO site switching on both of the surfaces as found in the experiments: at low coverages, bridge species is formed on the surface, and at high coverages, NO switches to atop sites.

1. Introduction

The interaction of NO with metal surfaces is an interesting chemical system for several reasons. The catalytic reduction of the NO_x species to N_2 is one of the important reactions that take place on automobile three-way catalysts. NO is also an important byproduct in the ammonia oxidation process. An understanding of chemisorption and heterogeneous catalysis on metal surfaces requires a detailed knowledge of adsorbate structure with respect to the substrate.[1] Structure sensitivity is another interesting topic of surface science and catalysis.[2] Heats of adsorption and local bonding geometries have been investigated not only experimentally but also theoretically,[3,4] and the review on NO adsorption up to 2000 has been given by Brown et al.[5] They have pointed out that the chemistry of NO is much more complex than that of CO, and that NO adsorbs in many different binding geometries because of the presence of a single unpaired electron in the antibonding $2\pi^*$ orbital. An extensive range of vibrational frequencies has been observed, and the assignment of vibrational peaks is found to be difficult because the transferability of the vibrational frequencies of nitrosyl compounds is questionable.

In this work, we deal with the adsorption of NO on Pt(110) surface as part of a continuing effort to understand the adsorption of NO on transition metal surfaces by density functional theory (DFT) method at the generalized gradient approximation (GGA) level.[6,7] A clean surface of Pt(110) is reconstructed to the (1×2) phase with a missing row, and the adsorption of NO or CO leads to lifting of this reconstruction to the (1×1) phase, depending on both coverage and surface temperature. Previous studies of NO on Pt(110) have been reviewed well by Brown et al.[5] and will be also discussed in detail later. Adsorption is mainly molecular, and only a small amount of dissociation, possibly on defect sites, is observed. The bridge NO species is seen on the surface at low coverage, and with increasing coverage NO is forced to occupy atop sites at saturation coverage. The vibrational spectra are quite complex and very dependent on both coverage and surface temperature. Ge et al. have performed DFT calculation of NO on Pt(110)-(1×1) and (1×2) with pseudopotential and plane-wave basis set.[8] On both of the surface phases, the most stable adsorption site is the bridge site on the edge of the close-packed row, and the atop site is less stable at all of the coverages investigated. The bridge NO species always adsorbs upright with its molecular axis normal. Tilting either along or perpendicular to the close-packed row causes a decrease in adsorption energy. On the atop sites, the most stable configuration is a polymeric $(NO)_x$ chain, and they have proposed that this may be the species observed experimentally at high coverages on the (1×2) surface, whereas this species is energetically less favorable than the bridge species. Their calculated vibrational frequencies are all higher than the experimental stretching frequencies up to ca. 200 cm^{-1}.

We have investigated adsorption energies and structures of NO on Pt(110) surface with full-geometry optimization and without symmetry restriction, and compared them with the experimental data. The assignment of adsorption sites has been carried out with precise calculation of vibrational frequencies for NO on various sites. We clearly show the NO site switching with increasing coverage as found in the experiments.

2. Computational Methods

DFT calculations were performed with the program package DMol^3 in Materials Studio (version 2.2) of Accelrys Inc. on personal computers. In the DMol^3 method,[9−11] the physical wave functions are expanded in terms of accurate numerical basis sets. We used the double-numeric quality basis set with polarization functions (DNP). The size of the DNP basis set is comparable to Gaussian 6-31 G**, but the DNP is more accurate than the Gaussian basis set of the same size. The gradient-corrected GGA functional, developed by Perdew, Burke, and Ernzerhof (PBE),[12] was employed. A Fermi smearing of 0.002

* Corresponding author. Phone: +81-29-861-4835. Fax: +81-29-861-9291. E-mail: hideo-orita@aist.go.jp.
† AIST, Tsukuba Central 5.
‡ AIST, Onogawa.

10.1021/jp050808b CCC: $30.25
Published on Web 04/26/2005

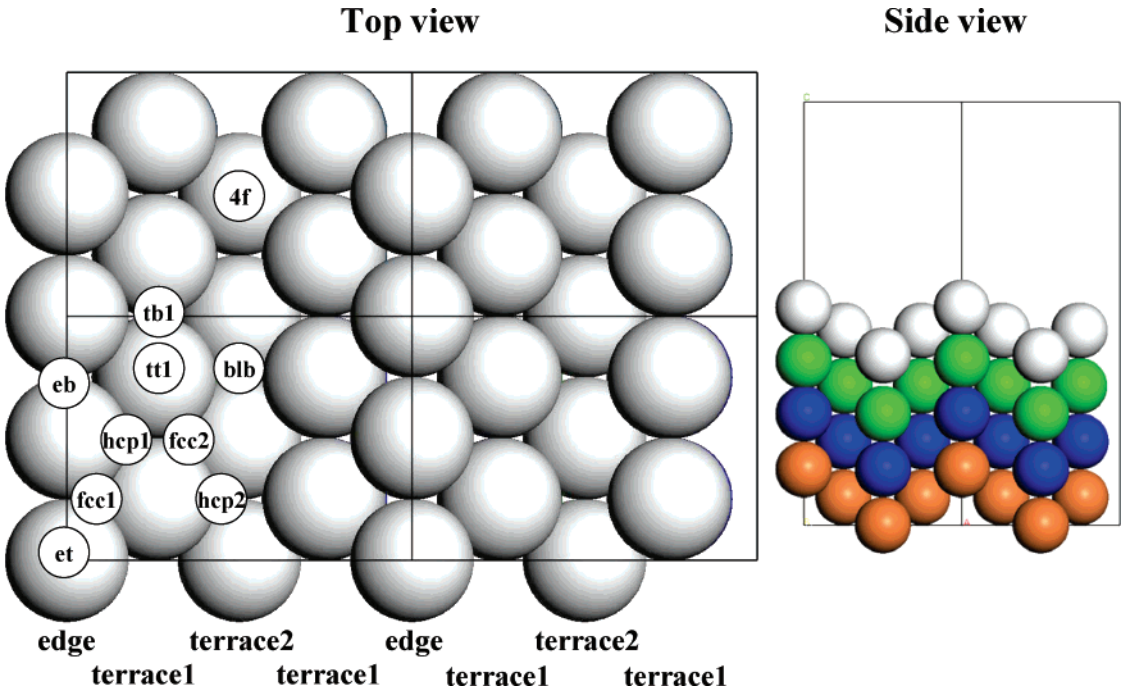

Figure 1. (Left) Illustration of adsorption sites on the reconstructed missing row (110) surface with the (2×2) unit lattice. The metal rows on the surface are classified into three types of edge, terrace1, and terrace2 by coordinate numbers of 7, 9, and 11, respectively. Adsorption sites are abbreviated as follows: et, atop site on the edge; eb, bridge site parallel to the edge; fcc1, fcc hollow site between the edge and terrace1 (terrace1 refers to the terrace near the edge); hcp1, hcp hollow site between the edge and terrace1; tt1, atop site on terrace1; tb1, bridge site between two terrace1 atoms; fcc2, fcc hollow site between terrace1 and terrace2 (terrace2 refers to the terrace at the bottom); hcp2, hcp hollow site between terrace1 and terrace2; blb, long-bridge site at the bottom; 4f, quasi 4-fold hollow site at the bottom. (Right) Side view of the reconstructed missing row (110) surface with the unit lattice.

hartree (1 hartree = 27.2114 eV) and a real-space cutoff of 4 Å were used to improve computational performance. Periodic surface slabs of 4 physical layers' thickness were used, with a 10 Å of vacuum region between the slabs. Adsorbate and the two top layers of metal were allowed to relax in all of the geometry optimization calculations without symmetry restriction (i.e., always using $P1$ symmetry). The tolerances of energy, gradient, and displacement convergence were 2×10^{-5} hartree, 4×10^{-3} hartree/Å, and 5×10^{-3} Å, respectively. The maximum gradient for most of the optimized structures was less than 2×10^{-3} hartree/Å. All of the geometry optimization calculations were carried out with spin polarization. Although all of the chemisorbed NO lost its spin identity, the N−O and Pt−N distances became longer at least by 0.01 Å in no-spin-polarized calculations. These small definite distance changes induced the differences of computed vibrational frequencies as much as 100 cm^{-1}. Adsorption energies were computed by subtracting the energies of the gas-phase NO molecule and surface from the energy of the adsorption system as shown in eq 1.

$$E_{ad} = E(\text{NO/surface}) - E(\text{NO}) - E(\text{surface}) \qquad (1)$$

With this definition, a negative E_{ad} corresponds to stable adsorption on the surface.

The experimentally determined Pt lattice constant of 3.924 Å was used for the production of the surfaces. All electron scalar relativistic (AER)[13] calculations were performed, because we have shown in the previous work on CO on Pt(111)[14] that AER calculations were essential to obtain the same site preference as inferred in experiments. Delley has reported an error for Pt bulk lattice constant as −0.41%.[15] Gil et al.[16] have checked the effect of using the experimental lattice constant, instead of the commonly used optimized value for the bulk. They have concluded that there is no significant effect on the difference in adsorption energy between atop and hollow sites. For the numerical integration, we used the XFINE quality mesh size of the program, which is a nearly saturated mesh for benchmark calculations. The tolerance of SCF convergence was 1×10^{-7}. Under the present computational conditions, the N−O bond length for free NO molecule was calculated as 1.164 Å, in good agreement with the experimental value of 1.151 Å.[17] The bond energy was calculated as 7.63 eV. The value also agrees well with the reported one (7.45 eV[18]).

Harmonic vibrational frequencies were calculated with displacing not only the NO molecules but also the first layer Pt atoms of surfaces as described in detail previously.[6] To reduce the computationally expensive cost of frequency calculation, density functional semicore pseudopotentials (DSPPs)[15] were employed instead of AER for spin-polarized AER-geometry-optimized structures without spin-polarization. Under the present calculational conditions, the harmonic frequency of free NO molecule (d(N−O) = 1.164 Å) was calculated as 1895 cm^{-1}. This value is only 0.5% smaller than the experimental harmonic value of 1904 cm^{-1}, and close to the anharmonic one (1876 cm^{-1}).

Two surface models, which are a reconstructed missing row phase and an unreconstructed phase, were adopted. A reconstructed missing row (2×2) surface unit cell (including 32 Pt atoms) was chosen to model adsorption of NO on the reconstructed surface with the coverages of $^1/_8$, $^1/_4$, and $^3/_8$ monolayer (one monolayer means that on top of each atom in the first physical layer a molecule is positioned). A 4×3×1 k-point sampling was used. Ten adsorption sites shown in Figure 1 and parallel adsorption configurations were investigated. On the other hand, an unreconstructed (2×1) surface unit cell (including 16 Pt atoms) was chosen to model adsorption of NO on the unreconstructed surface with the coverages of $^1/_4$ and $^1/_2$

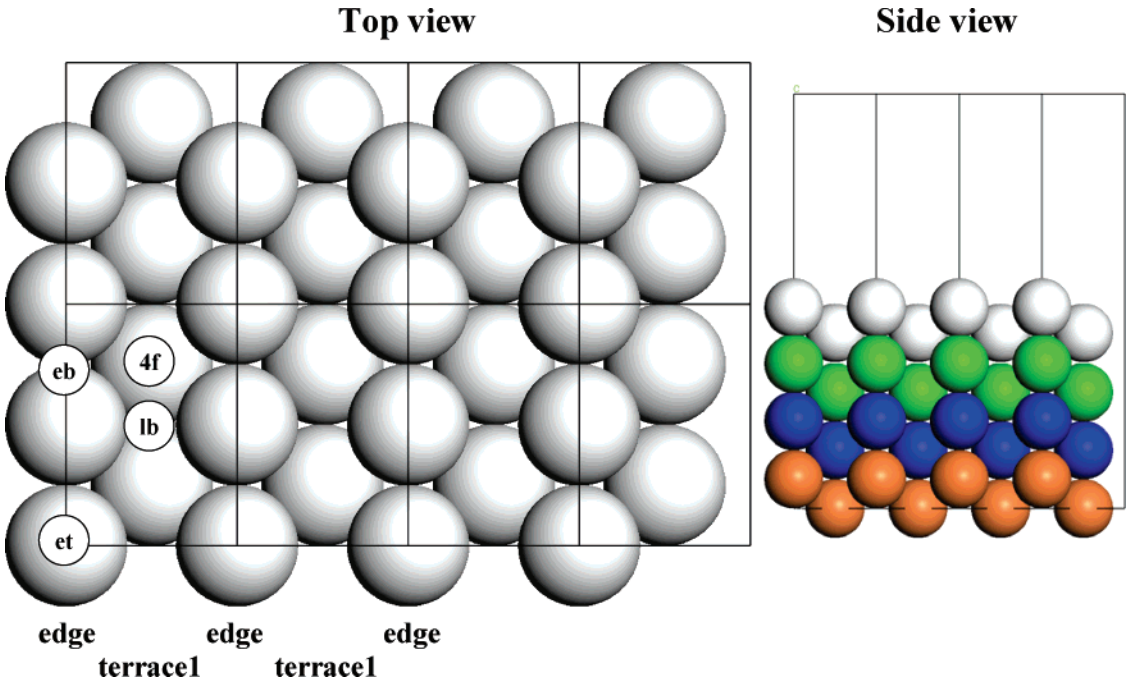

Figure 2. (Left) Illustration of adsorption sites on the unreconstructed (110) surface with the (2×1) unit lattice. The metal rows on the surface are classified into two types of edge and terrace1 by coordinate numbers of 7 and 11, respectively. Adsorption sites are abbreviated as follows: et, atop site on the edge; eb, bridge site parallel to the edge; lb, long-bridge site at the bottom; 4f, quasi 4-fold hollow site at the bottom. (Right) Side view of the unreconstructed (110) surface with the unit lattice.

monolayer. A 4×5×1 k-point sampling was used. Only four adsorption sites shown in Figure 2 were investigated.

3. Results and Discussion

We have calculated adsorption energies, structures, and N−O stretching vibrational frequencies of NO on Pt(110) at several coverages with two different surface models: metastable reconstructed (2×2) and unreconstructed (2×1) surface unit cells. The calculated adsorption energies, structures, and vibrational frequencies are listed in Table 1. Typical optimized adsorption structures for NO on Pt(110) are shown in Figures 3−5. The most favorite adsorption at $^1/_8$ monolayer in the reconstructed missing row (2×2) unit cell occurs at the eb site with E_{ad} of −2.17 eV (for abbreviation of adsorption sites, see the caption of Figure 1). The energy difference from the second favorite site of p-eb (parallel adsorption over eb; lying geometry along the edge with the center of mass over eb and the atoms oriented toward et) is 0.14 eV. The third favorite adsorption occurs at the et site with E_{ad} of −1.99 eV. The et NO species tilts considerably, and its polar/azimuthal angles are 39.2°/−33.6°. The blb site is locally stable and is the fourth favorite site with E_{ad} of −1.85 eV, which is equal or larger than the adsorption energies of the sites on the (111) microfacets (fcc1, −1.85 eV; hcp1, −1.73 eV; tt1, −1.66 eV; tb1, −1.65 eV). The two Pt atoms that are attaching to NO move closer together considerably. The fcc2 and 4f sites are unstable, and the NO molecules move to the tb1 and blb sites, respectively. When the adsorption of NO is simulated from the initial adsorption site of hcp2, geometry optimization leads to an interesting activated adsorption structure with a positive E_{ad} of 0.12 eV. The N−O bond length stretches up to 1.26 Å, and the oxygen atom goes close to the Pt atom on the other side of (111) microfacet with a d(Pt−O) of 2.24 Å. The N−O stretching frequency becomes smaller up to 1251 cm^{-1}. Although there is considerable confusion whether the dissociation of NO on Pt(110) occurs[19,20] or not,[21] this activated adsorption structure might be a candidate for decomposition intermediate.

King and co-workers have measured the adsorption heat of NO on Pt(110) calorimetrically[22] (it should be noted that in the papers of King and co-workers,[3,4,5,8,22,23] a differently defined monolayer is used, and their defined monolayer equals twice that of ours in the present work). The initial heat of adsorption at 300 K is 1.66 eV and remains constant (within errors) for the first 0.1−0.125 monolayer. Adsorption heat then drops abruptly to 1.45 eV and again remains constant up to 0.335 monolayer, before dropping steeply toward the reversible value of 0.98 eV. Our calculated adsorption energies are a little large in comparison with the experimental results because of the tendency of overestimation in the DFT methods.[3,4]

According to the RAIRS experiments[23] at 90 K, where lifting of the (1×2) reconstruction to the (1×1) phase as well as multilayer formation is inhibited, Brown et al. have found that initial adsorption leads the appearance of a single peak at 1599 cm^{-1}, which shifts up to 1610 cm^{-1} with increasing coverage. The peak position is in good agreement with the calculated harmonic frequency (1625 cm^{-1}) for the eb NO species at $^1/_8$ monolayer. Therefore, the eb species is formed first on the surface and dominant at the low coverage. The tilt angle of the adsorbed NO at the eb site is calculated as 0.06° from the surface normal. Brown et al. also have proposed that adsorbed NO at the eb site is upright at the low coverage.

For the coverages of $^1/_4$ and $^3/_8$ monolayer, several configurations of the adsorbed NO in the reconstructed missing row (2×2) unit cell have been investigated by considering the sum of adsorption energies at $^1/_8$ monolayer and local geometries between the NO adsorbates. The most favorite adsorption configuration at $^1/_4$ monolayer is the eb+blb with E_{ad} of −2.02 eV/NO. The energy differences from the second and third favorite configurations of et+blb and 2et are 0.10 and 0.11 eV/NO, respectively. The configuration of 2eb becomes the least stable with E_{ad} of −1.80 eV/NO, whereas the eb site is most stable at $^1/_8$ monolayer. The two bridge NO species tilt slightly, and the polar angles from the (110) normal are calculated as 4.9° and 4.5°. With increasing NO exposure to 0.37 L (1 L

TABLE 1: Adsorption Energies, Structures, and Stretching Frequencies for NO on Pt(110) Surface in Reconstructed Missing Row (2×2) and Unreconstructed (2×1) Unit Cells

ad site	E_{ad}[a]/eV	d(Pt−N)/Å	d(N−O)/Å	angle[b]/deg	ν(NO)/cm^{-1}
		Reconstructed Missing Row (2 × 2)			
		$^1/_8$ Monolayer			
et	−1.99	1.83	1.17	39.2, −33.6	1758
eb	−2.17	1.97, 1.97	1.19	0.06, 0	1625
fcc1	−1.85	2.07, 2.08, 2.08	1.21	28.1, 90	1506
hcp1	−1.73	2.08, 2.10, 2.10	1.21	27.5, 90	1531
tt1	−1.66	1.94	1.17	45.7, −1.7	1697
tb1	−1.65	1.97, 1.97	1.19	30.3, 90	1636
fcc2		not stable: move to tb1			
hcp2	0.12	1.91, 2.10, 2.11, (2.24)[c]	1.26	34.1, 89.5	1251
blb	−1.85	2.04, 2.04	1.19	0, 0	1621
4f		not stable: move to blb			
p-eb	−2.03	1.88, (2.20)[c]	1.23	82.5, −0.04	1362
		$^1/_4$ Monolayer			
2et	−1.91	1.85	1.17	56.4, −68.0	1761, 1684
		1.86	1.18	54.3, 53.1	
2eb	−1.80	1.94, 1.94	1.19	4.9, 90.3	1701, 1587
		1.94, 1.94	1.19	4.5, 89.5	
et+blb	−1.92	et: 1.81	1.17	31.5, −28.1	1804, 1601
		blb: 2.03, 2.03	1.19	2.0, 179.3	
eb+blb	−2.02	eb: 1.97, 1.97	1.19	2.9, −96.1	1646, 1602
		blb: 2.04, 2.04	1.19	1.1, 90.0	
		$^3/_8$ Monolayer			
2et+blb	−1.90	et: 1.84	1.17	49.2, −109.1	1779, 1702
		1.84	1.18	50.9, 65.2	1582
		blb: 2.03, 2.04	1.19	1.9, 1.9	
2eb+blb	−1.83	eb: 1.96, 1.96	1.19	8.1, −90.3	1686, 1590
		1.97, 1.97	1.19	7.9, 90.4	1583
		blb: 2.02, 2.06	1.19	1.1, 102.2	
2eb+tb1	−1.78	eb: 1.96, 1.96	1.20	7.2, 102.8	1692, 1623
		1.94, 1.95	1.19	11.4, −75.8	1587
		tb1: 1.96, 1.98	1.19	28.8, 91.7	
		Unreconstructed (2 × 1)			
		$^1/_4$ Monolayer			
et	−2.11	1.84	1.18	44.7, 16.0	1721
eb	−2.35	1.97, 1.97	1.19	0.1, 93.9	1656
p-eb	−2.25	1.89, (2.17)[c]	1.23	84.0, 0.03	1351
lb		not stable: move to et			
4f		not stable: move to eb			
		$^1/_2$ Monolayer			
2et	−1.91	1.86	1.18	50.7, −57.4	1774, 1649
		1.86	1.18	50.8, 48.7	
2eb	−1.85	1.94, 1.94	1.19	3.8, 89.9	1720, 1595
		1.94, 1.94	1.19	3.4, 90.1	

[a] Adsorption energy per NO molecule. [b] Polar angle of the N−O axis from the (110) normal, and azimuthal angle of the N−O axis from the Pt edge row. [c] d(Pt−O).

(Langmuir) = 1 × 10^{-6} mbar s), RAIR spectra of Brown et al.[23] show that a second NO peak develops at 1620 cm^{-1}, which grows in intensity and shifts up to 1626 cm^{-1}, whereas the first peak at 1610 cm^{-1} decreases in intensity. For the eb+blb configuration, the N−O stretching frequencies are calculated as 1646 cm^{-1} (symmetric mode and dipole active being visible in IR measurements: two NO molecules vibrate in the same direction) and 1602 cm^{-1} (antisymmetric mode: two NO molecules vibrate in the opposite directions). Therefore, the second peak at 1620−1626 cm^{-1} is due to the eb+blb configuration, and the peak at 1610 cm^{-1}, which comes from isolated NO at the eb site, is diminishing with increasing NO coverage on the surface.

The most stable configuration at $^3/_8$ monolayer is the 2et+blb with E_{ad} of −1.90 eV/NO. The two atop NO species tilt alternately. Their polar/azimuthal angles are 49.2°/−109.1° and 50.9°/65.2°, whereas the blb species adsorbs almost upright (1.9°/1.9°). Comparing with 2et configuration at $^1/_4$ monolayer, the magnitude of the polar and azimuthal angle becomes smaller and larger, respectively, in the presence of the blb species. The calculated N−O stretching frequencies of this configuration are 1779 cm^{-1} (symmetric mode and dipole active being visible in IR measurements: three NO molecules vibrate in the same direction, but the two et NO species vibrate more largely than the blb species), 1702 cm^{-1} (antisymmetric mode; the two et species mainly vibrate in the opposite directions), and 1582 cm^{-1} (antisymmetric mode; the blb species mainly vibrates). The second favorite configuration is the 2eb+blb (the energy difference from the 2et+blb configuration is 0.07 eV/NO), and its calculated N−O stretching frequencies are 1686 cm^{-1} (symmetric mode and dipole active being visible in IR measurements: three NO molecules vibrate in the same direction), 1590 cm^{-1} (antisymmetric mode), and 1583 cm^{-1} (antisymmetric mode). At high coverages, Brown et al.[23] have observed that the higher frequency peak at ca. 1760 cm^{-1} dominates as the peaks in the 1610−1635 cm^{-1} region decrease in intensity and that a further peak at ca. 1690 cm^{-1} grows in at the saturation coverage. The peaks at ca. 1760 and 1690 cm^{-1} can be assigned due to the 2et+blb and 2eb+blb configurations, respectively. At the saturation coverage, the less stable configuration of

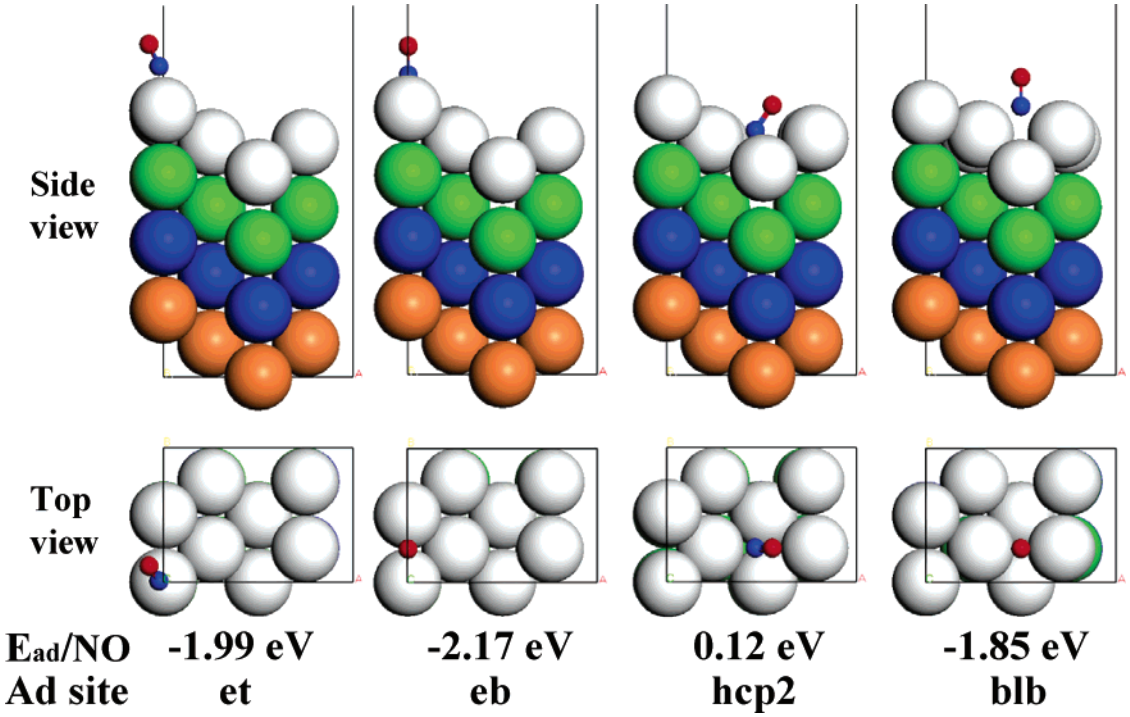

Figure 3. Typical adsorption structures of NO on Pt(110) at $^1/_8$ monolayer in the reconstructed missing row (2×2) unit cell.

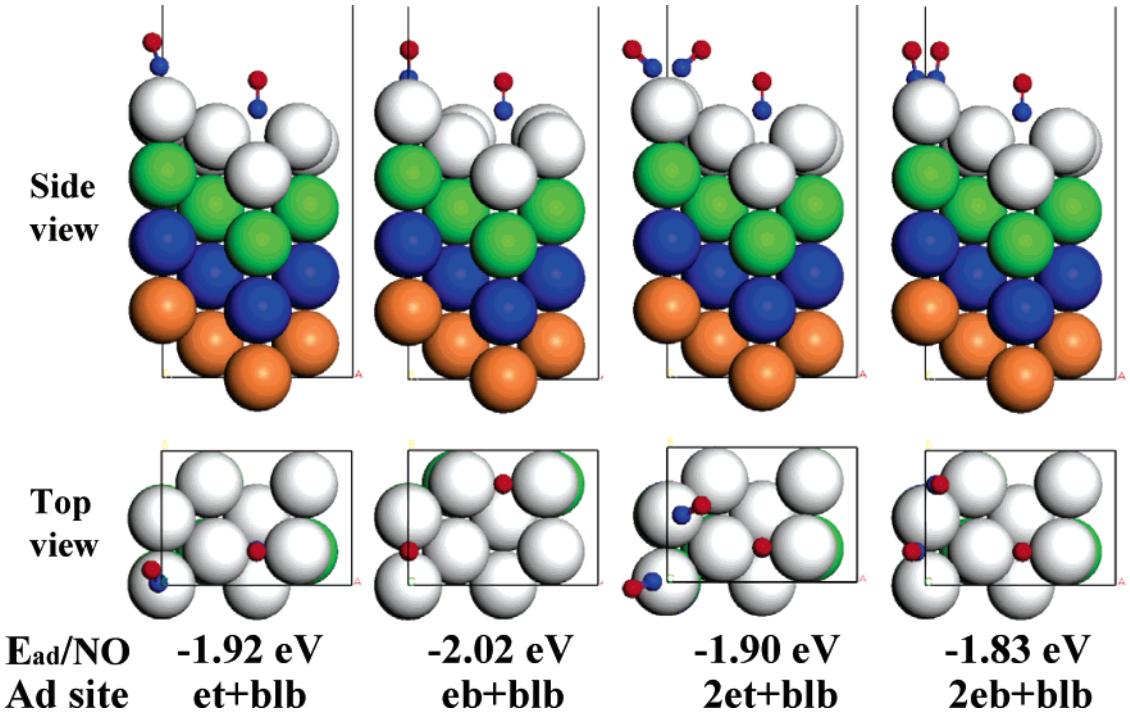

Figure 4. Typical adsorption structures of NO on Pt(110) at $^1/_4$ and $^3/_8$ monolayer in the reconstructed missing row (2×2) unit cell.

2eb+blb is probably also populated at low temperature. In fact, there is no peak at ca. 1690 cm^{-1} for RAIR spectra at 230 K.[23]

For the unreconstructed (2×1) unit cell, the most favorite adsorption at $^1/_4$ monolayer occurs at the eb site with E_{ad} of −2.35 eV. The energy differences from the second and third favorite site of p-eb and et are 0.10 and 0.25 eV, respectively. The lb and 4f sites are unstable for the unreconstructed (2×1) unit cell, and the NO molecules move to the et and eb sites through the three-fold hollow sites near edge (hcp1 and fcc1), respectively. Therefore, the hcp1 and fcc1 sites are also unstable. The NO species at the eb site adsorbs upright (the polar angle is only 0.1°). The calculated N−O stretching frequency is 1656 cm^{-1}. This frequency is a little larger than that for the eb species at $^1/_8$ monolayer in the reconstructed (2×2) unit cell (1625 cm^{-1}).

The most favorite adsorption at $^1/_2$ monolayer for the unreconstructed (2×1) unit cell occurs at the et site with E_{ad} of −1.91 eV/NO. The two et NO species tilt alternately, and their polar/azimuthal angles are 50.7°/−57.4° and 50.8°/48.7°. The structure of 2et NO species at $^1/_2$ monolayer corresponds to the ordered (2×1)-p1g1-NO structure as observed by Jackman et al.[24] This ordered, high coverage structure can be obtained by annealing the substrate at ca. 600 K and cooling in an NO ambient. The inability to form the ordered (2×1)-p1g1 structure

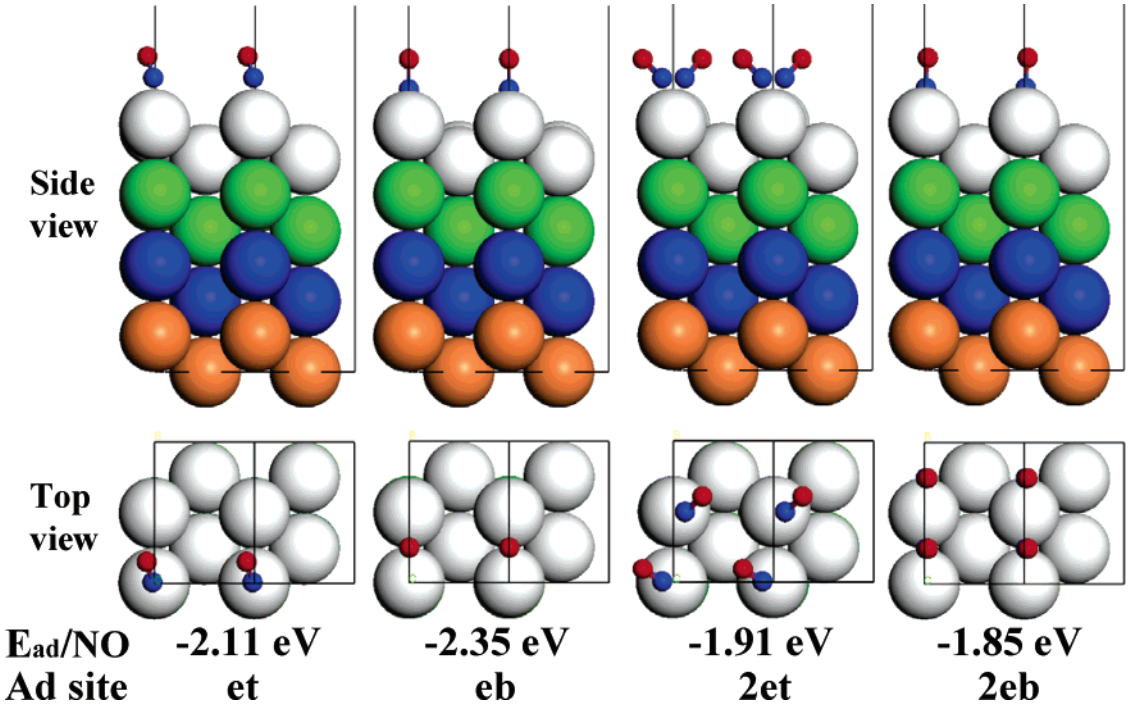

Figure 5. Typical adsorption structures of NO on Pt(110) at $^1/_4$ and $^1/_2$ monolayer in the unreconstructed (2×1) unit cell. Two unit cells are shown to compare with adsorption structures in the reconstructed (2×2) unit cell.

at room temperature has been attributed to the imperfect lifting of the reconstruction. The calculated N−O stretching frequencies are 1774 cm^{-1} (symmetric mode) and 1649 cm^{-1} (antisymmetric mode). The 2eb configuration is less stable, although the energy difference from the 2et configuration is 0.06 eV/NO. The two eb NO species adsorb almost upright, and the polar angles are only 3.8° and 3.4°. The calculated N−O stretching frequencies are 1720 cm^{-1} (symmetric mode) and 1595 cm^{-1} (antisymmetric mode).

From the RAIRS measurements at 300 K,[23] where lifting of (1×2) reconstruction to the (1×1) phase occurs with increasing coverage, Brown et al. have indicated that bridge NO species is initially formed, which is replaced with increasing coverage by atop NO, and that there are three peaks at 1796 cm^{-1} (dominant), 1712 cm^{-1} (middle), and 1613 cm^{-1} (very weak, and almost diminishing) at the saturation coverage. The peaks at 1796 and 1712 cm^{-1} can be assigned due to the 2et and 2eb configurations at $^1/_2$ monolayer, respectively. At the saturation coverage, the less stable configuration of 2eb is probably also populated as the energy difference is only 0.06 eV/NO. The peak at 1610 cm^{-1}, which comes from isolated NO at the eb site in the reconstructed (2×2) unit cell, is diminishing with increasing NO coverage on the surface. The present calculational results interpret the RAIR spectra of Brown et al.[23] very well from the low to the saturation coverages.

Comparing the adsorption energies of NO at $^1/_4$ monolayer between the reconstructed missing row (2×2) and unreconstructed (2×1) unit cells, the adsorption energy in the unreconstructed (2×1) unit cell is 0.33 eV/NO larger than that in the reconstructed missing row (2×2) unit cell. On the other hand, we have found that without NO adsorption the reconstructed (2×2) unit cell is more stable than the unreconstructed (2×1) unit cell by 0.17 eV/(2×1) surface unit cell. Therefore, the adsorption of NO at $^1/_4$ monolayer should lead to lifting of Pt(110) surface to the unreconstructed phase because the total energy becomes more stable by 0.16 eV/(2×1) unit cell for the unreconstructed phase than the reconstructed phase because of NO adsorption.

Brown et al. have also examined the adsorption of NO at 30 K up to very high coverage (i.e., physisorbed multilayers).[25] At this low temperature, diffusion of NO across the surface is suppressed and metastable adsorbate species are formed. Initially, peaks appear at ca. 1600 and ca. 1350 cm^{-1}, and these are closely followed by weaker peaks peak at 1670 and 1560−1570 cm^{-1}. With higher NO exposure, additional peaks grow in at 1730 and 1864 cm^{-1}, and the initial peak at 1600 cm^{-1} disappears. The very intense peaks at 1778 and 1864 cm^{-1} are assigned due to the physisorbed NO dimers, $(NO)_2$, adsorbed above the chemisorbed layer. After annealing an adlayer formed at 30 K, containing both chemisorbed and physisorbed NO, to 130 K, only one peak is seen at 1760 cm^{-1}. On the other hand, after annealing an adlayer containing only chemisorbed NO, two infrared peaks at 1773 and 1632 cm^{-1} are observed. Brown et al. have concluded that the physisorbed overlayer partially incorporates into the chemisorbed layer to produce an unusually dense layer, whereas they did not check the coverage of NO directly with TPD or other methods. From the present calculational results, however, this phenomenon does not seem unusual. The peak at 1760−1773 cm^{-1} is assigned due to the 2et+blb configuration at $^3/_8$ monolayer, and the peak at 1632 cm^{-1} is due to the eb+blb configuration at $^1/_4$ monolayer. The appearance of two peaks after annealing an adlayer containing only chemisorbed NO comes from a little smaller initial coverage, which is not enough to produce the 2et+blb configuration on the whole surface. The peak at 1350 cm^{-1} has been assigned to the three-fold site on the (111) microfacet (i.e., hcp1) by Brown et al.,[25,26] but the frequency for the hcp1 species is calculated as 1531 cm^{-1} in the present work. The peak position is rather close to that for the p-eb species (1362 cm^{-1}), but this species is lying almost parallel to the edge, and its peak intensity for RAIRS should become weak. Although the p-eb species is the second favorite in the reconstructed (2×2) unit cell and may be formed because of the suppression of the diffusion, we cannot assign the peak at 1350 cm^{-1} definitely at present. The candidate for the peak at 1670 cm^{-1} is the tt1 (1697 cm^{-1}) or tb1 (1636 cm^{-1}) species, but the adsorption energies of these species are

a little smaller (−1.66 and −1.65 eV). The peak at 1560−1570 cm^{-1} may be assigned to the hcp1 species. The assignment of the RAIR spectra measured at low temperatures is rather difficult, because the diffusion of adsorbate across the surface is suppressed, and the adsorbate might be trapped at defect sites on the surface.

Recently, we have investigated CO adsorption on Pt(110)-(1×2) and (1×1) surfaces with the same DFT method.[27] There are several striking differences between NO and CO adsorption as follows. First, the most favorite adsorption site at low coverages for NO is the eb site instead of the et for CO, and only for coverages larger than $^3/_8$ monolayer NO molecule begins to adsorb at the et site. The adsorption site switching is clearly observed experimentally for NO as demonstrated theoretically in the present work: at low coverages, bridge species is formed on the surface, and at high coverages, NO switches to atop species. For CO, the et site is always most stable up to $^1/_2$ monolayer. Second, tilt angle of NO is much more dependent on adsorption site and coverage than that of CO. Especially, the atop NO species tilts more largely than the atop CO. Third, the blb site is relatively more stable for NO. The difference of adsorption energy from the most favorite site at $^1/_8$ monolayer in the reconstructed (2×2) unit cell is 0.32 eV for NO, but 0.42 eV for CO. The most stable configuration at $^1/_4$ monolayer in the reconstructed (2×2) unit cell is the eb+blb configuration for NO instead of the 2et for CO. Fourth, the ordered structure on the unreconstructed (1×1) surface is (2×1)-p1g1 for NO, but (2×1)-p2mg for CO. Fifth, the parallel adsorption over the eb is locally stable for NO. Sixth, the difference of stretching frequency between the atop and bridge species is smaller for NO (ca. 100 cm^{-1} (sometimes less than 60 cm^{-1}) for NO and ca. 200 cm^{-1} for CO), so more careful investigation is necessary for NO.

4. Conclusion

Adsorption of NO on Pt(110)-(1×2) and (1×1) surfaces has been investigated by density functional theory (DFT) method (periodic DMol[3]) at the generalized gradient approximation (GGA) level with full geometry optimization and without symmetry restriction. Adsorption energies, structures, and N−O stretching vibrational frequencies of NO are studied by considering multiple possible adsorption sites and comparing with the experimental data. Adsorption is strongly dependent on both coverage and surface phase. The assignment of adsorption sites can be carried out with precise calculation of vibrational frequencies for NO on various sites. We clearly show the NO site switching on both of the surfaces as found in the experiments: at low coverages, bridge species is formed on the surface, and at high coverages, NO switches to atop sites. Two atop species tilt alternately at high coverages, and the structure of two atop species at $^1/_2$ monolayer in the unreconstructed (2×1) unit cell corresponds well to the ordered (2×1)-p1g1-NO structure observed by LEED. The unreconstructed (1×1) surface is more stable than the reconstructed (1×2) surface when NO adsorbs on the surface. The present calculational results interpret the RAIR spectra of Brown et al.[23] very well from the low to the saturation coverages.

References and Notes

(1) Somorjai, G. A. *Introduction to Surface Chemistry and Catalysis*; Wiley: New York, 1994.
(2) Matsushima, T. *Surf. Sci. Rep.* **2003**, *52*, 1.
(3) Brown, W. A.; Kose, R.; King, D. A. *Chem. Rev.* **1998**, *98*, 797.
(4) Ge, Q.; Kose, R.; King, D. A. *Adv. Catal.* **2000**, *45*, 207 and references therein.
(5) Brown, W. A.; King, D. A. *J. Phys. Chem. B* **2000**, *104*, 2578.
(6) Orita, H.; Nakamura, I.; Fujitani, T. *Surf. Sci.* **2004**, *571*, 102.
(7) Orita, H.; Nakamura, I.; Fujitani, T. *J. Chem. Phys.* **2005**, *122*, 014703.
(8) Ge, Q.; Brown, W. A.; Sharma, R. K.; King, D. A. *J. Chem. Phys.* **1999**, *110*, 12082.
(9) Delley, B. *J. Chem. Phys.* **1990**, *92*, 508.
(10) Delley, B. *J. Phys. Chem.* **1996**, *100*, 6107.
(11) Delley, B. *J. Chem. Phys.* **2000**, *113*, 7756.
(12) Perdew, J. P.; Burke, K.; Ernzerhof, M. *Phys. Rev. Lett.* **1996**, *77*, 3865.
(13) Delley, B. *Int. J. Quantum Chem.* **1998**, *69*, 423.
(14) Orita, H.; Itoh, N.; Inada, Y. *Chem. Phys. Lett.* **2004**, *384*, 271.
(15) Delley, B. *Phys. Rev. B* **2002**, *66*, 155125.
(16) Gil, A.; Clotet, A.; Ricart, J. M.; Kresse, G.; García-Hernández, M.; Rösch, N.; Sautet, P. *Surf. Sci.* **2003**, *530*, 71.
(17) *CRC Handbook of Chemistry and Physics*, 81st ed.; Lide, D. R., Ed.; CRC Press: Boca Raton, FL, 2000.
(18) Kurth, S.; Perdew, J. P.; Blaha, P. *Int. J. Quantum Chem.* **1999**, *75*, 889.
(19) Comrie, C. M.; Weinberg, W. H.; Lambert, R. M. *Surf. Sci.* **1976**, *57*, 619.
(20) Gorte, R. J.; Gland, J. L. *Surf. Sci.* **1981**, *102*, 348.
(21) Freyer, N.; Kiskinova, M.; Pirug, G.; Bonzel, H. P. *Appl. Phys. A* **1986**, *39*, 209.
(22) Wartnaby, C. E.; Stuck, A.; Yeo, Y. Y.; King, D. A. *J. Phys. Chem.* **1996**, *100*, 12483.
(23) Brown, W. A.; Sharma, R. K.; King, D. A. *J. Phys. Chem.* **1998**, *102*, 5303.
(24) Jackman, T. E.; Davies, J. A.; Jackson, D. P.; Unertl, W. N.; Norton, P. R. *Surf. Sci.* **1982**, *120*, 389.
(25) Brown, W. A.; Sharma, R. K.; Ge, Q.; King, D. A. *Phys. Chem. Chem. Phys.* **1999**, *1*, 1995.
(26) Brown, W. A.; Ge, Q.; Sharma, R. K.; King, D. A. *Chem. Phys. Lett.* **1999**, *299*, 253.
(27) Yamagishi, S.; Fujimoto, T.; Inada, Y.; Orita, H. *J. Phys. Chem. B*, in press.